Supporting Information

Lignosulfonate biomass derived N and S co-doped porous carbon for efficient oxygen reduction reaction

Mingli Zhang [a,†], Yanliang Song [b,†], Hengcong Tao [a], Chao Yan [c], Justus Masa [d], Yongchao Liu [c], Xiaoyou Shi [b], Shizhen Liu [a], Xu Zhang [b,*], Zhenyu Sun [a,*]

[a] *State Key Laboratory of Organic-Inorganic Composites, Beijing University of Chemical Technology, Beijing 100029, China. E-mail: sunzy@mail.buct.edu.cn*

[b] *Beijing Key Lab of Bioprocess, College of Life Science and Technology, Beijing University of Chemical Technology, Beijing 100029, China*

[c] *School of Material Science & Engineering, Jiangsu University of Science and Technology, Zhenjiang 212003, China*

[d] *Analytische Chemie-Elektroanalytik & Sensorik, Ruhr-University Bochum, 44780 Bochum, Germany*

[e] *Department of Chemistry, Kyambogo University, P.O. Box 1, Kyambogo (Kampala), Uganda*

† These authors contributed equally to this work.

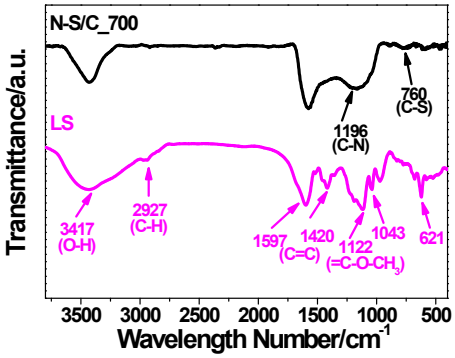

Fig. S1. FTIR spectra of original lignosulfonate (LS) and N-S/C_700. Characteristic anti-symmetry and symmetry stretching vibrations of sulfonic group (1043 cm^{-1} and 621 cm^{-1}), O-H (3417 cm^{-1}), C-H (2927 cm^{-1}), C=C (1597 cm^{-1} and 1420 cm^{-1}), and =C-O-CH_3 (1122 cm^{-1}) were observed in the LS [1].

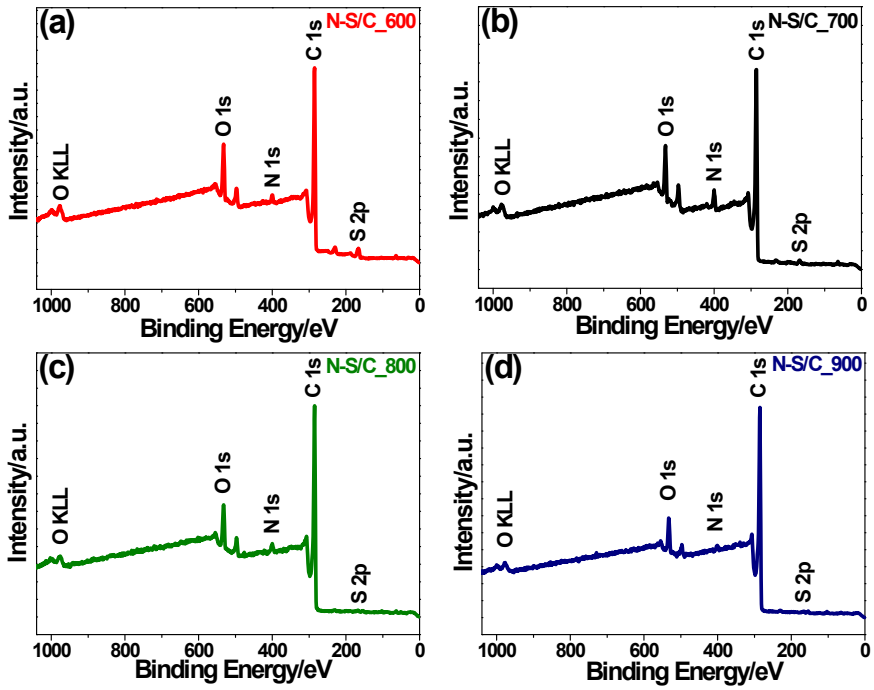

Fig. S2. Wide-survey XPS spectra of (a) N-S/C_600, (b) N-S/C_700, (c) N-S/C_800, and (d) N-S/C_900.

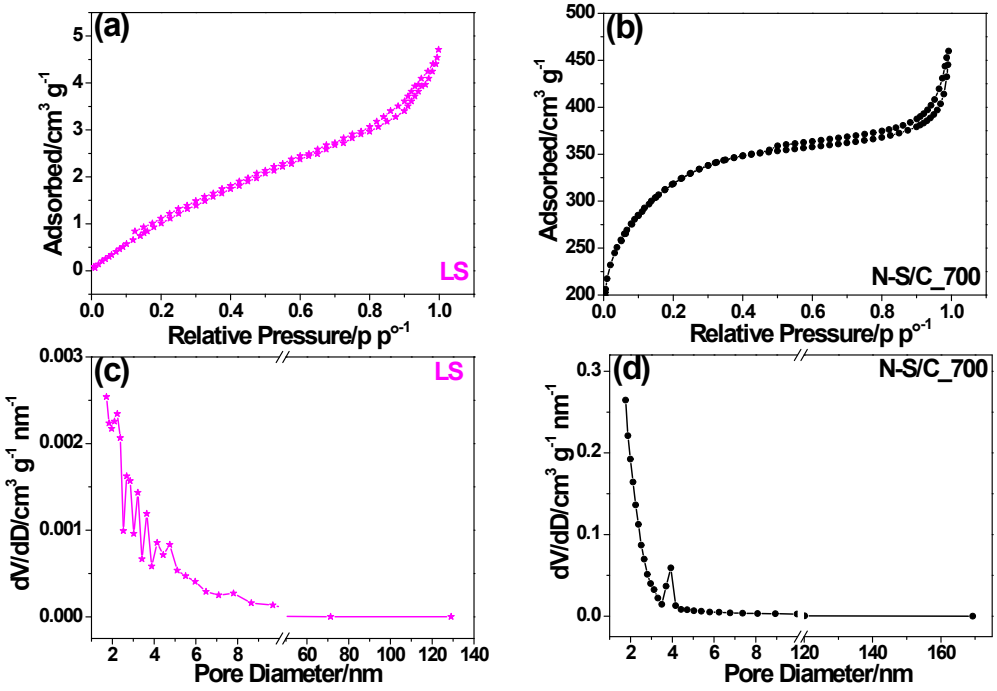

Fig. S3. Nitrogen sorption isotherms of (a) LS and (b) N-S/C_700 at 77 K. Pore size distribution profiles of (c) LS and (d) N-S/C_700.

Table S1. Porosity parameters of original lignosulfonate (LS) and N-S/C_700

		Pore Volume/$cm^3\ g^{-1}$			
Sample	**$S_{BET}/m^2\ g^{-1}$**	**$V_{tot.}$**	**$V_{micro.}$**	**$V_{meso.}$**	**Pore Size/nm**
LS	7.2	0.0073	0.0028	0.0045	3.49
N-S/C_700	1165.44	0.71	0.27	0.44	3.89

Table S2. Electrochemical activity parameters of the N-S/C_700 catalyst and some reported carbon materials for the ORR

Catalyst	**$E_{1/2}$ (V *vs.* RHE)**	**E_{onset} (V *vs.* RHE)**	**Rotation Rate (rpm)**	**J (mA cm^{-2})**	**Reference**	**Ref. (Year)**
N-S/C-700	0.75	0.80	400	2.86	Our work	
PNCP	0.73	0.80	400	2.3	Carbon	[2] (2018)
NC-1000	0.68	0.78	1600	3.6	Adv. Funct. Mater.	[3] (2018)
N/S-CNF	0.58	0.70	1600	4.2	Carbon	[4] (2016)
N/S-2DPC-60	0.75	0.83	1600	4.7	Adv. Funct. Mater.	[5] (2016)
PAC-5S	0.792	0.83	1600	6.19	J. Mater. Chem. A	[6] (2016)
NS-3DrGO-950	0.732	0.89	1600	5.23	Carbon	[7] (2017)
NS-G	0.665	0.81	1600	2.1	Adv. Mater.	[8] (2014)
NS-GP	0.642	0.78	1600	3.72	ACS Appl. Mater. Interfaces	[9] (2016)

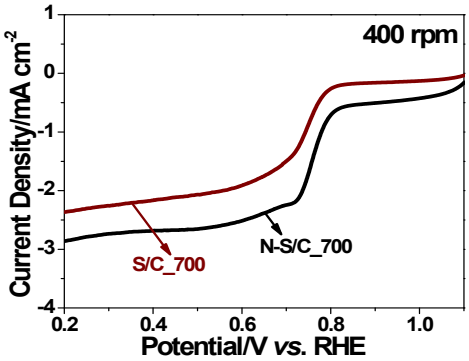

Fig. S4. LSVs of LS annealed at 700 °C (S/C_700) and N-S/C_700 recorded at 400 rpm in O_2-saturated aqueous KOH (0.1 M).

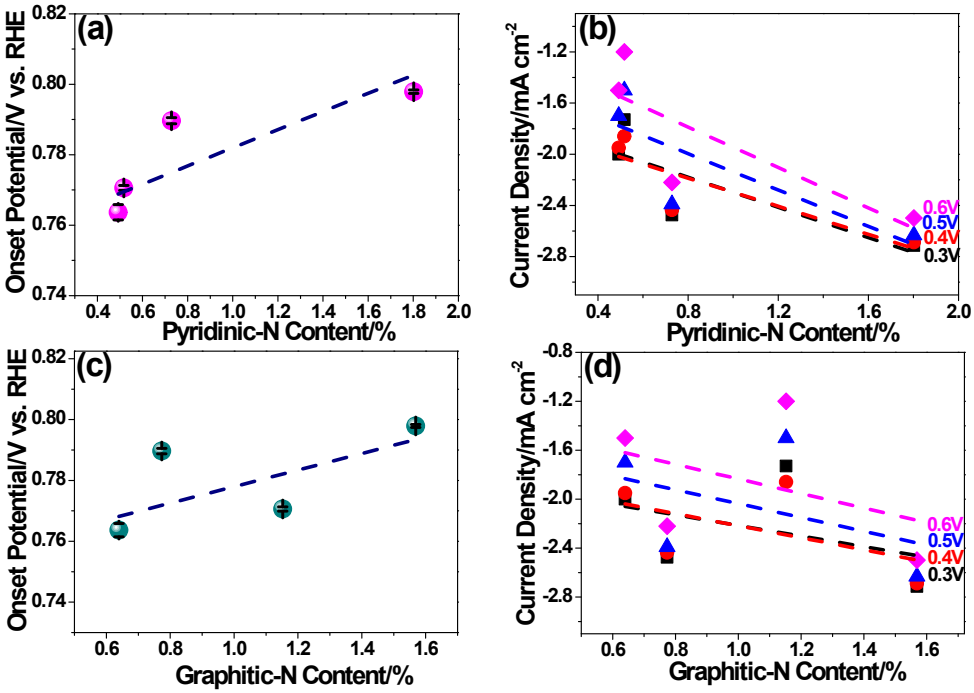

Fig. S5. Correlation of onset potential with content of (a) pyridinic nitrogen and (c) graphitic nitrogen. Correlation of current density (0.3 V, 0.4 V, 0.5 V and 0.6 V vs. RHE) with content of (b) pyridinic nitrogen and (d) graphitic nitrogen.

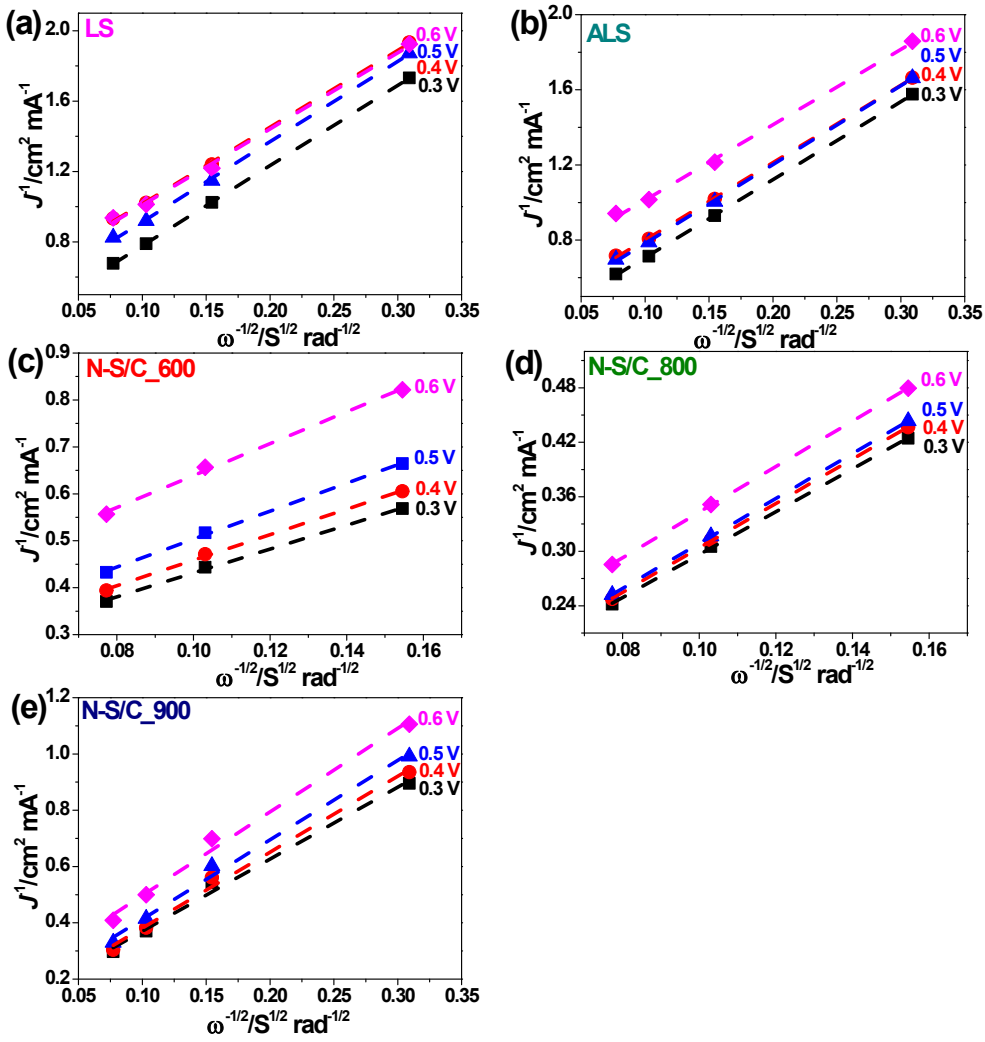

Fig. S6. Koutecky-Levich plots of (a) LS, (b) ALS, (c) N-S/C_600, (d) N-S/C_800, and (e) N-S/C_900.

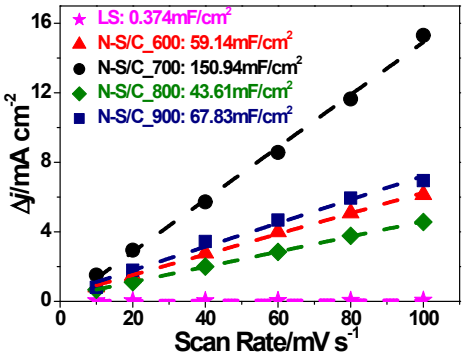

Fig. S7. Current density of CV experiments of LS, N-S/C_600, N-S/C_700, N-S/C_800, and N-S/C_900 at 0.65 V (*vs*. RHE) as a function of scan rate. The slope of each line shows the double layer capacitor of corresponding catalyst.

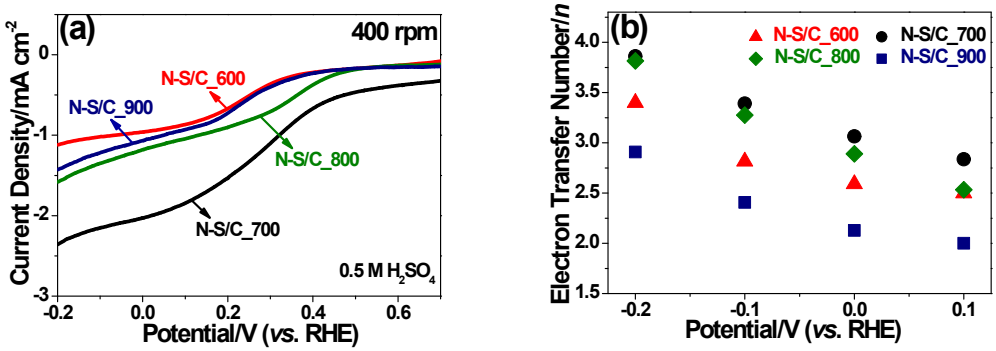

Fig. S8. (a) LSVs of N-S/C_600, N-S/C_700, N-S/C_800, and N-S/C_900 recorded at 400 rpm and 5 mV s^{-1} in oxygen-saturated H_2SO_4 (0.5 M). (b) Number of electrons transferred for N-S/C_600, N-S/C_700, N-S/C_800, and N-S/C_900 derived from the LSV results.

References

[1] Y. Wang, X. Wang, Y. Ding, Z. Zhou, C. Hao, S. Zhou, Novel sodium lignosulphonate assisted synthesis of well dispersed Fe_3O_4 microspheres for efficient adsorption of copper (II), Power Technology 325 (2018) 597-605.

[2] Z.Y. Sui, X. Li, Z.Y. Sun, H.C. Tao, P.Y. Zhang, L. Zhao, B.H. Han, Nitrogen-doped and nanostructured carbons with high surface area for enhanced oxygen reduction reaction, Carbon 126 (2018) 111-118.

[3] M. Qiao, S.S. Meysami, G.A. Ferrero, F. Xie, H. Meng, N. Grobert, M.M. Titirici, Low-cost chitosan-derived N-doped carbons boost electrocatalytic activity of multiwall carbon nanotubes, Adv. Funct. Mater. (2018) 1707284.

[4] T. Liu, Y.F. Guo, Y.M. Yan, F. Wang, C. Deng, D. Rooney, K.N. Sun, CoO nanoparticles embedded in three-dimensional nitrogen/sulfur co-doped carbon nanofiber networks as a bifunctional catalyst for oxygen reduction/evolution reactions, Carbon 106 (2016) 84-92.

[5] Y. Su, Z. Yao, F. Zhang, H. Wang, Z. Mics, E. Canovas, M. Bonn, X. Zhuang, X. Feng, Sulfur-enriched conjugated polymer nanosheet derived sulfur and nitrogen co-doped porous carbon nanosheets as electrocatalysts for oxygen reduction reaction and zinc–air battery, Adv. Funct. Mater. 26 (2016) 5893-5902.

[6] C. You, X. Jiang, L. Han, X. Wang, Q. Lin, Y. Hua, C. Wang, X. Liu, S. Liao, Uniform nitrogen and sulphur co-doped hollow carbon nanospheres as efficient metal-free electrocatalysts for oxygen reduction, J. Mater. Chem. A. 5 (2017) 1742-1748.

[7] Y. Li a, J. Yang, J. Huang, Y. Zhou, K. Xu, N. Zhao, X. Cheng, Soft template-assisted method for synthesis of nitrogen and sulfur co-dope d three-dimensional reduced graphene oxide as an efficient metal free catalyst for oxygen reduction reaction, Carbon 122 (2017) 237-246.

[8] W. Ai, Z. Luo, J. Jiang, J. Zhu, Z. Du, Z. Fan, L. Xie, H. Zhang, W. Huang, T. Yu, Nitrogen and sulfur codoped graphene: multifunctional electrode materials for high-performance li-ion batteries and oxygen reduction reaction, Adv. Mater. 26 (2014) 6186-6192.

[9] T. Akhter, M.M. Islam, S.N. Faisal, E. Haque, A.I. Minett, H.K. Liu, K. Konstantinov, S.X. Dou, Self-assembled N/S codoped flexible graphene paper for high performance energy storage and oxygen reduction reaction, ACS Appl. Mater. Interfaces 8 (2016) 2078-2087.